

generation of heat and no formation of a complex, consistent with the observations noted above. Upon addition of  $\text{AgO}_3\text{SCF}_3$  to solutions of **3**, heat was evolved (ca. 16 kcal mol<sup>-1</sup>) until two equivalents of metal were added. This is consistent with the formation of complex  $[\mathbf{3} \cdot \text{Ag}_2]^{2+}$ . The addition of  $\text{AgO}_3\text{SCF}_3$  to dodecamer **4** also resulted in the generation of heat, but no defined end point was reached due to the lower association constant. These results indicate that the addition of phenylacetylene segments that cannot bind metals to **2** allows for metal–ligand coordination to occur and shows that solvophobic interactions play a role in the metal-induced formation of the helical structure.

In conclusion, our results demonstrate that the oligomer sequence **1** can be modified to tightly and selectively bind metal ions in the internal cavity of a helical structure. The strength of metal ion binding appears to be derived from a combination of solvophobic interactions that favor the helical structure along with the more usual metal–ligand interactions.

Received: August 7, 1998 [Z12267IE]

German version: *Angew. Chem.* **1999**, *111*, 245–249

**Keywords:** conformation analysis • coordination chemistry • helical structures • oligomers • supramolecular chemistry

- [17] D. Venkataraman, Y. Du, S. Wilson, K. Hirsch, P. Zhang, J. Moore, *J. Chem. Ed.* **1997**, *74*, 915.
- [18] Similar behavior is observed for solutions of **3** with  $\text{Cu}^+$  salts, but not with  $\text{Cu}^{2+}$  salts. This is explained by the ability of  $\text{Cu}^+$  ions to adopt trigonal-planar coordination environments, while  $\text{Cu}^{2+}$  ions prefer a square-planar or octahedral bonding geometry.
- [19] Additional evidence for the stoichiometry of metal binding is provided by ESI-MS. The major peak is assigned to a doubly charged species corresponding to  $[\mathbf{3} \cdot \text{Ag}_2]^{2+}$ .
- [20] The NMR spectra of **3** are similar to those of **5**, but there are twice as many resonances.
- [21] K. Wuthrich, *NMR of Proteins and Nucleic Acids*, Wiley, New York, **1986**.
- [22] The addition of less than two equivalents of  $\text{AgO}_3\text{SCF}_3$  to a solution in THF results in broad, undefined signals in the aromatic region, characteristic of a system that is fluctuating on the NMR time scale.
- [23] K. A. Connors, *Binding Constants: The Measurement of Molecular Complex Stability*, Wiley, New York, **1987**.
- [24] The UV/Vis spectra showed a clear isobestic point at 375 nm, indicative of only one species being formed upon complexation.

## Peptide Folding: When Simulation Meets Experiment

Xavier Daura, Karl Gademann, Bernhard Jaun, Dieter Seebach, Wilfred F. van Gunsteren,\* and Alan E. Mark

The last two decades have seen the horizons of science and engineering being expanded greatly by the use of computer simulation techniques. In particular, computer simulation is the method of choice to study processes that are dangerous, costly, or even impossible to carry out experimentally, or that are of microscopic nature and thereby partially inaccessible to detailed observation. Molecular dynamics (MD) simulations, in which Newton's equations of motion are integrated to reproduce the time evolution (trajectory) of the atoms in a system, are widely used to study dynamic processes in biomolecular systems at atomic resolution.<sup>[1]</sup>

The ultimate goal of any simulation is to characterize and predict the behavior of real systems. Whether this goal is achieved depends on the quality of the model used and the computational power available. No model is an exact representation of the real system. All models must be verified, normally by comparison to experimental data. In the case of simulations aimed at understanding the mechanism of peptide or protein folding, verification represents a significant challenge. First, the dynamics of individual atoms during the process of folding cannot yet be directly observed experimentally. Experimental data at atomic resolution is only available for equilibrium distributions of conformations under

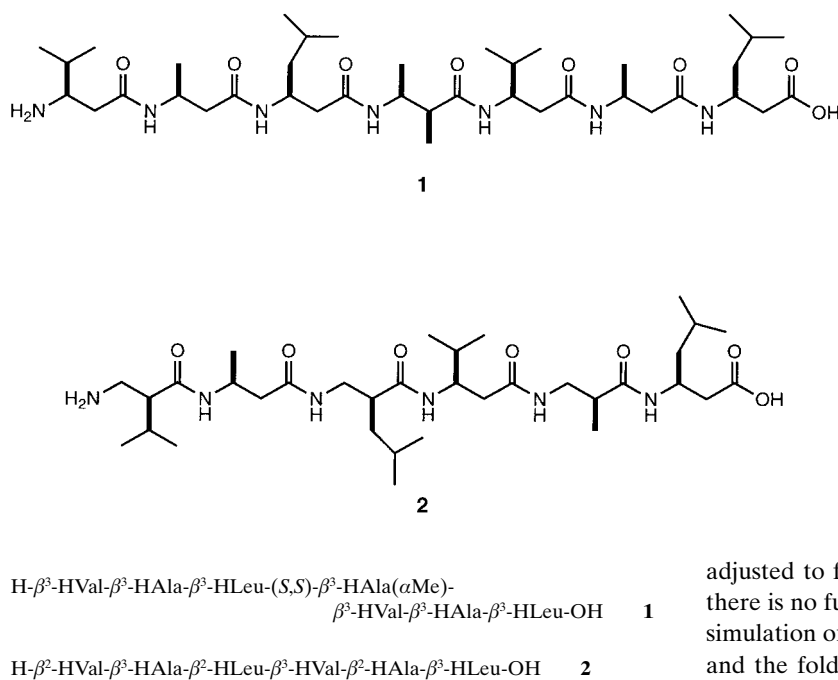
- [1] S. H. Gellman, *Acc. Chem. Res.* **1998**, *31*, 173–180.
- [2] J. L. Matthews, D. Seebach, *Chem. Commun.* **1997**, 2015–2022.
- [3] Y. Hamuro, S. J. Geib, A. D. Hamilton, *J. Am. Chem. Soc.* **1997**, *119*, 10587–10593.
- [4] R. S. Lokey, B. L. Iverson, *Nature* **1995**, *375*, 303–305.
- [5] D. Bassani, J.-M. Lehn, G. Baum, D. Fenske, *Angew. Chem.* **1997**, *109*, 1931–1933; *Angew. Chem. Int. Ed. Engl.* **1997**, *36*, 1845–1847.
- [6] A. Rigault, J. Siegel, J. Harrowfield, B. Chevrier, D. Moras, J.-M. Lehn, *Proc. Natl. Acad. Sci. USA* **1987**, *84*, 2566–2569.
- [7] T. M. Garrett, U. Koert, J.-M. Lehn, A. Rigault, D. Meyer, J. Fischer, *J. Chem. Soc. Chem. Commun.* **1990**, 557–558.
- [8] A. Williams, *Chem. Eur. J.* **1997**, *3*, 15–19.
- [9] C. Piquet, G. Bernardinelli, G. Hopfgartner, *Chem. Rev.* **1997**, *97*, 2005–2062.
- [10] J. C. Nelson, J. G. Saven, J. S. Moore, P. G. Wolynes, *Science* **1997**, *277*, 1793–1796.
- [11] A. Ben-Naim, *J. Phys. Chem.* **1971**, *54*, 1387–1404.
- [12] The solvophobically induced helical structure of **3** was characterized by the same methods as oligomers **1**. Solutions of **3** in acetonitrile provided helical structures, as indicated by <sup>1</sup>H NMR and UV/Vis spectroscopy. Thus, the secondary structure of **3** can be controlled using a solvophobic driving force, and the cyano groups on the interior of the tubular cavity do not appear to inhibit the formation of helical structures.
- [13] Oligomers **2**–**5** were shown to be pure by <sup>1</sup>H NMR spectroscopy, size-exclusion chromatography, high-performance liquid chromatography, and matrix-assisted laser desorption ionization mass spectrometry (MALDI-MS). Compounds **2** and **3** gave acceptable elemental analyses. Further details of the preparation and characterization of all compounds will be reported elsewhere.
- [14] For examples of preorganized, ion-binding systems substituted with cyano groups, see a) K. Pack, C. B. Knobler, E. F. Maverick, D. J. Cram, *J. Am. Chem. Soc.* **1989**, *74*, 8662–8671; b) Y. Tobe, N. Utsumi, A. Nagano, K. Naemura, *Angew. Chem.* **1998**, *110*, 1347–1349; *Angew. Chem. Int. Ed.* **1998**, *37*, 1285–1287.
- [15] R. H. P. Francisco, Y. P. Mascareñas, J. R. Lechat, *Acta Crystallogr. Sect. B* **1979**, *35*, 177–178.
- [16] L. Carlucci, G. Ciani, D. Prosperio, A. Sironi, *J. Am. Chem. Soc.* **1995**, *117*, 4562–4569.

\* Prof. Dr. W. F. van Gunsteren, Dr. X. Daura, Dr. A. E. Mark  
Laboratorium für Physikalische Chemie, ETH Zürich  
ETH-Zentrum, CH-8092 Zürich (Switzerland)  
Fax: (+41) 1-632-1039  
E-mail: wfvgn@igc.phys.chem.ethz.ch  
K. Gademann, Prof. Dr. B. Jaun, Prof. Dr. D. Seebach  
Laboratorium für Organische Chemie, ETH Zürich  
ETH-Zentrum, CH-8092 Zürich (Switzerland)

specific conditions. Second, the time scale on which the relevant biomolecular systems can be simulated in atomic detail is currently on the order of picoseconds to nanoseconds, while the lower limit for proteins as well as most peptides to fold is believed to be microseconds. Third, the process of peptide folding involves many (peptide and solvent) degrees of freedom and is governed by small (free) energy differences, on the order of a few multiples of  $k_B T$  ( $k_B$  = Boltzmann's constant), which puts very high demands on the accuracy of the atomic interaction function and model that is used.

Here we show that reversible folding of peptides in solution in atomic detail has come within the reach of computer simulation. This is especially useful since peptides are highly flexible molecules for which little structural information can be obtained by experiment. Yet, their structures are highly relevant to their interactions in living organisms.

We present MD simulation studies on the folding of two  $\beta$ -peptides.  $\beta$ -Peptides are nonnatural peptides composed of  $\beta$ -amino acids ( $R^4-NH-C^{\beta}HR^3-C^{\alpha}HR^2-CO-R^1$ ).<sup>[2]</sup> They have recently attracted much attention due to their potential use as peptide mimetics which are stable to peptidases and whose conformation can be tuned by altering the position of the side chain.<sup>[2-6]</sup> The  $\beta$ -peptides studied were the  $\beta$ -heptapeptide **1** and the  $\beta$ -hexapeptide **2**.



In **1** all side chains are in position  $R^3$  (except for residue number four, which is methylated at both  $R^3$  and  $R^2$  positions), while in **2** the side chains alternate between positions  $R^2$  and  $R^3$ . In methanol and pyridine, **1** adopts a left-handed helix (hydrogen bonds between residues  $i$  and  $i+2$ ) consisting of three residues per turn ( $3_1$ -helix), in which the amide C=O bonds point in the direction of the N terminus (Figure 1a).<sup>[3]</sup> In the same solvents, **2** predominantly forms a right-handed helix (hydrogen bonds between residues  $i$  and  $i+1$ , and between  $i$  and  $i-3$ ) in which the amide C=O bonds point alternately up and down the helix axis (Figure 1b, c).<sup>[4, 5]</sup>

The folds of the  $\beta$ -hepta- and  $\beta$ -hexapeptides were modeled based on NMR data.<sup>[3-5]</sup> Slightly different structures for **2** in methanol (Figure 1b) and in pyridine (Figure 1c) were inferred. The NMR data obtained in pyridine could be fitted by a model in which the  $\beta$ -hexapeptide forms a regular helix with hydrogen bonds NH(3)-O(4), NH(4)-O(1), and NH(6)-O(3). A hydrogen bond is here considered to exist if the proton-acceptor distance is less than 0.25 nm and the donor-proton-acceptor angle is greater than 135°. To simultaneously satisfy all the distance constraints derived from the 34 NOEs detected in methanol, the  $\beta$ -hexapeptide is forced to adopt a distorted helix containing just one hydrogen bond, NH(4)-O(1) (Figure 1b). Three of the 34 NOEs are responsible for this distortion. The root mean square difference (RMSD) in atom position between the two model structures (Figures 1b, c) is 0.07 nm (backbone, residues 2–5).

For several reasons, these systems are well suited for the study of peptide folding by MD simulation. First, although the time scale on which they fold in methanol is not known experimentally, in simulations these peptides fold on a time scale of nanoseconds. This is fast when compared with small helix-forming  $\alpha$ -peptides in aqueous solution.<sup>[7]</sup> Second, methanol has a lower density than water, making it a computationally less expensive solvent (by a factor of about three) in which to simulate folding. Third,  $\beta$ -peptides can adopt a range of secondary-structure elements depending on the side-chain composition and position. The small differences in the sequences of the two peptides lead to two profoundly different folds (Figure 1), although Seebach and co-workers<sup>[4]</sup> had designed the  $\beta$ -hexapeptide to form the left-handed helix of the  $\beta$ -heptapeptide. Because the conformation is sensitive to the precise nature of the atomic interactions, the system is a very sensitive test case for the force field used in the simulations. It should be noted that the GROMOS96 force field<sup>[8]</sup> used in this work has not been developed for  $\beta$ -amino acids or  $\beta$ -peptides. Therefore, there can be no suspicion that the force field has been artificially adjusted to favor the experimentally observed folds. Finally, there is no fundamental difference between the study by MD simulation of the folding of these two  $\beta$ -peptides in methanol and the folding of a peptide composed of  $\alpha$ -amino acids in water, other than the time scale on which folding occurs and the time scale that can be simulated.

Figure 2 shows, as a function of time, the RMSD between the structures given in Figure 1, which represent the predominant conformation in solution at 298 K modeled based on experimental NMR data, and conformations sampled during the simulations at 340 K. For the  $\beta$ -heptapeptide **1** a particular conformation was considered to be folded if the RMSD was 0.1 nm or less (backbone, residues 2–6).<sup>[9]</sup> For the  $\beta$ -hexapeptide **2** a lower boundary of 0.08 nm (backbone, residues 2–5) was used in proportion with the number of residues in the two peptides. As can be seen from Figure 2, both **1** and **2** fold and

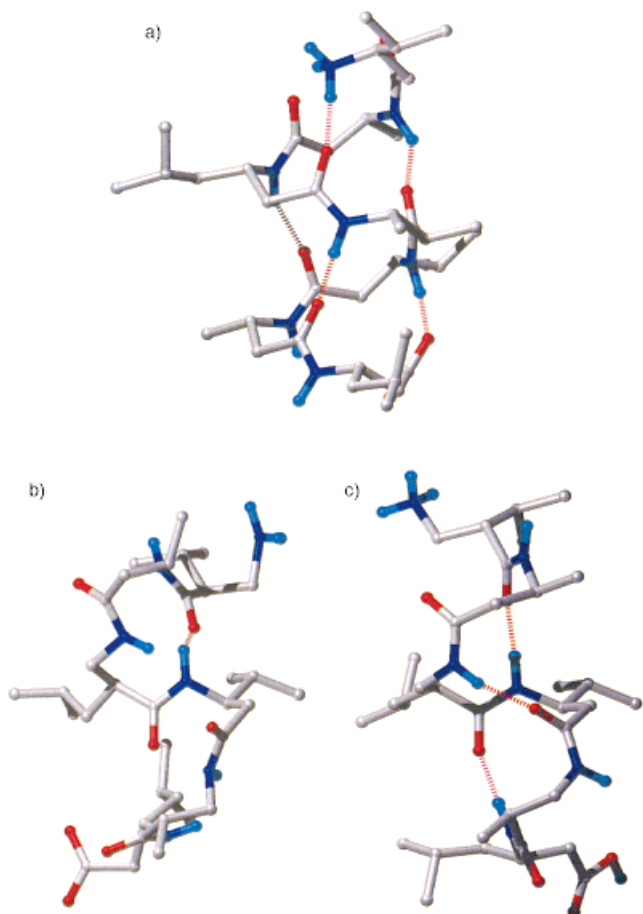


Figure 1. a) Molecular model for the  $\beta$ -heptapeptide **1** derived from NMR data obtained in methanol at 298 K.<sup>[3]</sup> b) Molecular model for the  $\beta$ -hexapeptide **2** derived from NMR data obtained in methanol at 298 K.<sup>[5]</sup> c) Molecular model for the  $\beta$ -hexapeptide **2** derived from NMR data obtained in pyridine at 298 K.<sup>[4]</sup> Hydrogen bonds (with a maximum proton–acceptor distance of 0.25 nm and a minimum donor–proton–acceptor angle of 135°) are shown with red dashed lines.

unfold several times during the 50 ns of simulation. In Figure 3 examples of folded and unfolded conformations from the simulations are shown. Although the simulation of **1** was initiated from the  $3_1$ -helical model structure, this peptide readily folds from a totally extended structure at 340 K.<sup>[9]</sup> The right-handed helical  $\beta$ -hexapeptide is clearly less stable than the left-handed helical  $\beta$ -heptapeptide at 340 K. The maximum lifetime observed for the left-handed helical  $\beta$ -heptapeptide conformation was on the order of 10 ns, while for the right-handed helical  $\beta$ -hexapeptide conformation it was on the order of 3 ns. Cluster analysis (see the Experimental Section) was performed using 5000 structures extracted from the trajectories at time intervals of 0.01 ns. For **1** the conformer represented by Figure 1a was the predominant conformer in the simulation, being populated approximately 50% of the time. In the case of **2** a single conformation did not so clearly dominate. Three clusters, including the most populated one, which together cover approximately 30% of the total ensemble would incorporate the conformation represented by Figure 1c. Interestingly, the left-handed  $3_1$ -helix was (approximately 1.3% of the time) among the

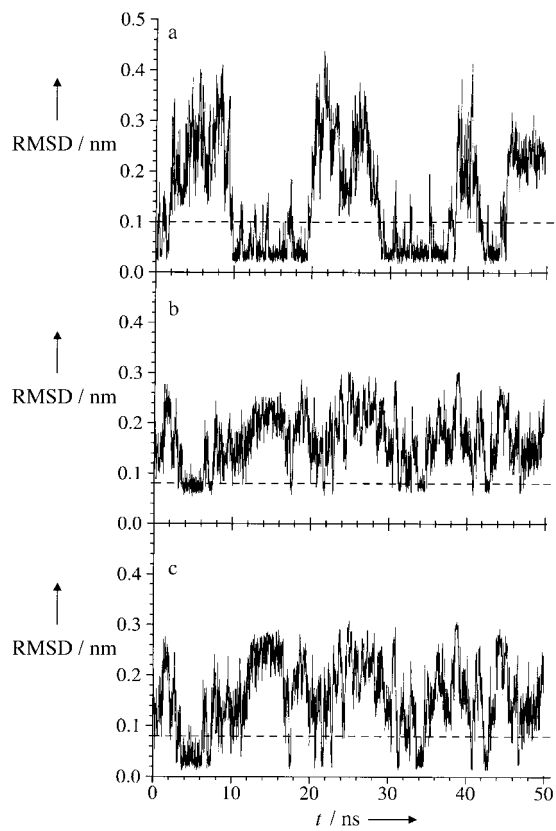


Figure 2. Backbone root-mean-square deviation (RMSD) of atom positions of the simulated structures from the model structures as a function of time at 340 K: a) RMSD from the model structure in Figure 1a for residues 2–6 of the  $\beta$ -heptapeptide **1**. b) RMSD from the model structure in Figure 1b for residues 2–5 of the  $\beta$ -hexapeptide **2** (0.33 nm for the initial (extended) structure). c) RMSD from the model structure in Figure 1c for residues 2–5 of the  $\beta$ -hexapeptide **2** (0.36 nm for the initial (extended) structure). Structures with an RMSD below the dashed lines have unequivocally the same fold as the model structures to which they are compared.

alternate conformations sampled by the  $\beta$ -hexapeptide during the simulation. By classification of all conformations with a backbone RMSD from the respective model structures of 0.10 nm (residues 2–6, **1**, Figure 2a) or 0.08 nm (residues 2–5, **2**, Figure 2c) as being folded and all conformations with an RMSD greater than 0.15 nm (**1**) or 0.12 nm (**2**) as being unfolded, the free energy of folding  $\Delta G_{\text{folding}}$  was estimated to be 0 and 4 kJ mol<sup>-1</sup> at 340 K for **1** and **2**, respectively.

The question of whether Figure 1b is an appropriate model for the most populated conformation of the  $\beta$ -hexapeptide **2** in methanol at room temperature can now be addressed. The simulation (Figure 2b, c) clearly suggests that Figure 1c represents a better model structure for **2** in methanol than Figure 1b. The conformation in Figure 1b is, in fact, high in energy in the force field due to both unfavorable bonded (bond angles, torsional angles) and nonbonded interactions, suggesting that such a conformation, even if it fulfills all the NOEs obtained in methanol, is improbable. More likely, the observed NOEs result from a mixture of two or more conformations in rapid equilibrium at 298 K. The three NOEs that are violated by the molecular model in Figure 1c are characteristic of a left-handed  $3_1$ -helix, and were not observed

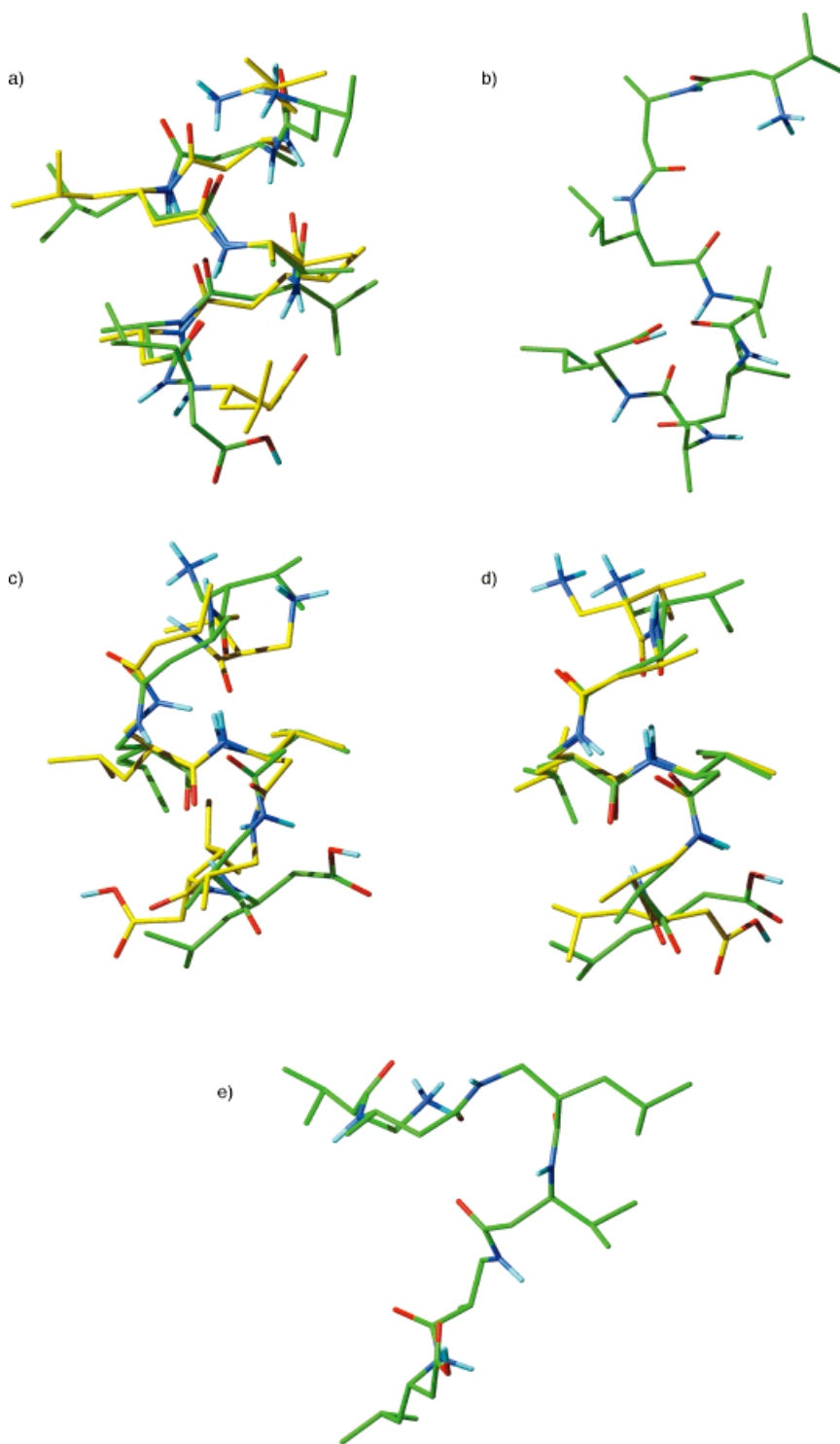


Figure 3. Selected conformations from the simulations: a) Superposition of the model structure in Figure 1a and the conformation of the  $\beta$ -heptapeptide **1** at time point 18 ns in the simulation [backbone RMSD of 0.03 nm (residues 2–6)]. b) Conformation of the  $\beta$ -heptapeptide **1** at time point 24 ns in the simulation [backbone RMSD of 0.25 nm (residues 2–6)]. c) Superposition of the model structure in Figure 1b and the conformation of the  $\beta$ -hexapeptide **2** at time point 5 ns in the simulation [backbone RMSD of 0.07 nm (residues 2–5)]. d) Superposition of the model structure in Figure 1c and the conformation of the  $\beta$ -hexapeptide **2** at time point 5 ns in the simulation [backbone RMSD of 0.02 nm (residues 2–5)]. e) Conformation of the  $\beta$ -hexapeptide **2** at time point 26 ns in the simulation [backbone RMSD from the model structures in Figure 1b, c of 0.21 nm (residues 2–5)].

in pyridine. The right-handed helical conformation of the  $\beta$ -hexapeptide was the predominant conformation in the simulation at 340 K. Nevertheless, several alternate conformations were also populated significantly, including a left-handed  $3_1$ -helix (1.3%). When averaged over the ensemble of conformations generated at 340 K using  $\text{NOE} \propto \langle 1/r^6 \rangle^{-1/6}$ , only one NOE observed in methanol is violated by more than 0.1 nm. Despite the fact that the results at 340 K cannot be directly related to the experimental results obtained at room temperature, it is clear that the right-handed helical conformation of the  $\beta$ -hexapeptide **2** is not as stable in methanol at 298 K as the left-handed helical conformation of the  $\beta$ -heptapeptide **1**, and alternate conformations, including perhaps the  $3_1$ -helix, account for some of the observed NOEs.

With this work we believe we have clearly demonstrated the ability to simulate in atomic detail the reversible folding of peptides in solution, albeit of non-natural  $\beta$ -peptides. Despite the small differences in sequence between the two peptides studied, the simulations correctly predict a left-handed  $3_1$ -helical fold for the  $\beta$ -heptapeptide and a right-handed helical fold for the  $\beta$ -hexapeptide. These results open a wide range of possibilities for the use of MD simulations in understanding the process of peptide folding and predicting possible folds of peptides in solution.

#### Experimental Section

Two 50-ns MD simulations at 340 K and 1 atm were performed for **1** and **2**. Periodic boundary conditions were applied. The initial structures were  $3_1$ -helical for **1** (Figure 1a) and extended (all backbone dihedral angles set to 180°) for **2**. The  $\beta$ -heptapeptide **1** was solvated with 962 methanol molecules in a rectangular box, and the  $\beta$ -hexapeptide **2** was solvated with 1435 methanol molecules in a truncated octahedron. In both cases the initial minimum distance between peptide and wall was chosen equal to the cut-off for the nonbonded interactions (1.4 nm). The temperature used for the simulations corresponds to the melting temperature of **1** in the force field, as estimated previously.<sup>[9]</sup> No restraints were applied. Parameter settings not commented here were as in reference [9]. The GROMOS96 package of programs and force field were used.<sup>[8]</sup>

To find clusters of structures in a trajectory the RMSD of atom positions between all pairs of structures was determined. For each structure the number of other structures for which the RMSD was 0.1 nm or less (backbone, residues 2–6) for **1** or 0.08 nm or less (backbone, residues 2–5) for **2**

(neighbor conformations) was calculated. The structure with the highest number of neighbors was taken as the center of a cluster, and formed together with all its neighbors a (first) cluster. The structures of this cluster were thereafter eliminated from the pool of structures. The process was repeated until the pool of structures was empty. In this way, a series of nonoverlapping clusters of structures was obtained.

Free energies of folding were calculated as  $\Delta G_{\text{folding}} = -k_B T \ln(p_{\text{folded}}/p_{\text{unfolded}})$ , where  $k_B$  is the Boltzmann constant,  $T$  is the temperature, and  $p_{\text{folded}}$  and  $p_{\text{unfolded}}$  are the relative probabilities of the folded and unfolded conformations;  $p_{\text{folded}}$  and  $p_{\text{unfolded}}$  are approximated by the number of folded and unfolded conformations sampled in the simulations.

Received: September 1, 1998 [Z 12359 IE]

German version: *Angew. Chem.* **1999**, *111*, 249–253

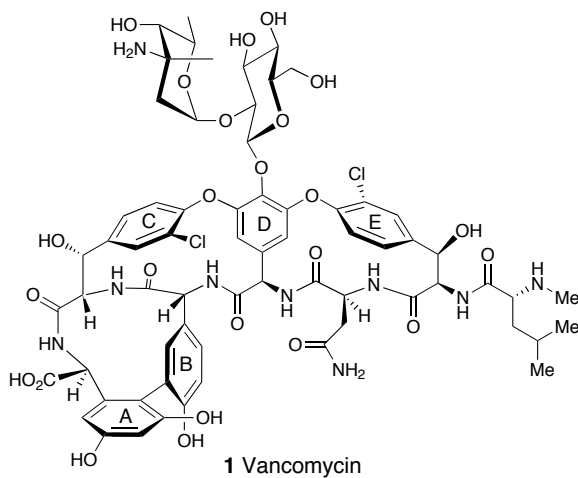
**Keywords:** computer chemistry • conformation analysis • molecular dynamics • peptide folding • peptides

- [1] *Computer simulation of biomolecular systems, theoretical and experimental applications*, Vols. 1–3 (Eds.: W. F. van Gunsteren, P. K. Weiner, A. J. Wilkinson), Kluwer, Dordrecht, **1989**–**1997**.
- [2] D. Seebach, M. Overhand, F. N. M. Kühnle, B. Martinoni, L. Oberer, U. Hommel, H. Widmer, *Helv. Chim. Acta* **1996**, *79*, 913–941.
- [3] D. Seebach, P. E. Ciceri, M. Overhand, B. Jaun, D. Rigo, L. Oberer, U. Hommel, R. Amstutz, H. Widmer, *Helv. Chim. Acta* **1996**, *79*, 2043–2066.
- [4] D. Seebach, K. Gademann, J. V. Schreiber, J. L. Matthews, T. Hintermann, B. Jaun, L. Oberer, U. Hommel, H. Widmer, *Helv. Chim. Acta* **1997**, *80*, 2033–2038.
- [5] D. Seebach, S. Abele, K. Gademann, G. Guichard, T. Hintermann, B. Jaun, J. L. Matthews, J. V. Schreiber, L. Oberer, U. Hommel, H. Widmer, *Helv. Chim. Acta* **1998**, *81*, 932–982.
- [6] a) T. Hintermann, D. Seebach, *Chimia* **1997**, *50*, 244–247; b) X. Daura, W. F. van Gunsteren, D. Rigo, B. Jaun, D. Seebach, *Chem. Eur. J.* **1997**, *3*, 1410–1417; c) D. H. Appella, L. A. Christianson, I. L. Karle, D. R. Powell, S. H. Gellman, *J. Am. Chem. Soc.* **1996**, *118*, 13071–13072; d) D. H. Appella, L. A. Christianson, D. A. Klein, D. R. Powell, X. Huang, J. J. Jr. Barchi, S. H. Gellman, *Nature* **1997**, *387*, 381–384; e) S. Krauthäuser, L. A. Christianson, D. R. Powell, S. H. Gellman, *J. Am. Chem. Soc.* **1997**, *119*, 11719–11720; f) S. H. Gellman, *Acc. Chem. Res.* **1998**, *31*, 173–180; g) S. Borman, *Chem. Eng. News* **1997**, *75*(24), 32–35; h) U. Koert, *Angew. Chem.* **1997**, *109*, 1922–1923; *Angew. Chem. Int. Ed. Engl.* **1997**, *36*, 1836–1837; i) B. L. Iverson, *Nature* **1997**, *385*, 113–115.
- [7] a) S. Williams, T. P. Causgrove, R. Gilman, K. S. Fang, R. H. Callender, W. H. Woodruff, R. B. Dyer, *Biochemistry* **1996**, *35*, 691–697; b) P. A. Thompson, W. A. Eaton, J. Hofrichter, *Biochemistry* **1997**, *36*, 9200–9210.
- [8] W. F. van Gunsteren, S. R. Billeter, A. A. Eising, P. H. Hünenberger, P. Krüger, A. E. Mark, W. R. P. Scott, I. G. Tironi, *Biomolecular Simulation: The GROMOS96 manual and user Guide*, Vdf Hochschulverlag AG an der ETH Zürich, Zürich, **1996**, pp. 1–1042.
- [9] X. Daura, B. Jaun, D. Seebach, W. F. van Gunsteren, A. E. Mark, *J. Mol. Biol.* **1998**, *280*, 925–932.

## Total Synthesis of Vancomycin\*\*

K. C. Nicolaou,\* Helen J. Mitchell,  
Nareshkumar F. Jain, Nicolas Winssinger,  
Robert Hughes, and Toshikazu Bando

Within the class of the glycopeptide antibiotics<sup>[1]</sup> vancomycin (**1**)<sup>[2]</sup> occupies a commanding position as a highly effective and widely used clinical agent for combating severe bacterial infections caused by drug resistant pathogens.<sup>[1–3]</sup> This novel



antibiotic, isolated from actinomycetes *Streptomyces orientalis* (later renamed *Nocardia orientalis* and finally reclassified as *Amycolatopsis orientalis*<sup>[2c]</sup>), has recently<sup>[3]</sup> moved to center stage by virtue of its increasing importance in chemistry, biology, and medicine. The total synthesis of this antibiotic has long been considered as a formidable challenge to synthetic organic chemistry.<sup>[4]</sup> Intense research efforts in recent times have culminated in the total synthesis of the vancomycin aglycon **2** (see Scheme 1), recently accomplished by the research group of Evans<sup>[5]</sup> and our own.<sup>[6]</sup> Herein we wish to report the total synthesis of vancomycin (**1**) itself. This synthesis involves sequential glycosidations of a suitably protected derivative of the previously synthesized vancomycin aglycon **2**<sup>[6]</sup> and delivers the target molecule in a highly efficient and stereoselective manner.

[\*] Prof. Dr. K. C. Nicolaou, H. J. Mitchell, Dr. N. F. Jain, N. Winssinger, R. Hughes, Dr. T. Bando  
Department of Chemistry and  
The Skaggs Institute for Chemical Biology  
The Scripps Research Institute  
10550 North Torrey Pines Road, La Jolla, CA 92037 (USA)  
Fax: (+1) 619-784-2469  
E-mail: kcn@scripps.edu  
and  
Department of Chemistry and Biochemistry  
University of California, San Diego  
9500 Gilman Drive, La Jolla, CA 92093 (USA)

[\*\*] We thank Dr. D. H. Huang and Dr. G. Siuzdak for NMR and mass spectrometric assistance, respectively. This work was financially supported by the National Institutes of Health (USA), The Skaggs Institute for Chemical Biology, and grants from Pfizer, Schering Plough, Hoffmann La Roche, and Merck.